agriculture

MDPI

Article

Mathematical Modeling of Heat and Mass Transfer during Moisture–Heat Treatment of Castor Beans to Improve the Quality of Vegetable Oil

Natalia Sorokova [1,*], Vladimir Didur [2] and Miroslav Variny [3]

[1] Scientific and Educational Institute of Atomic and Thermal Energy, National Technical University of Ukraine "Igor Sikorsky Kyiv Polytechnic Institute", Polytechnic 6, 02000 Kiev, Ukraine
[2] Department of Agricultural Engineering, Faculty of Engineering and Technology, Uman National University of Horticulture, 20300 Uman, Ukraine
[3] Department of Chemical and Biochemical Engineering, Faculty of Chemical and Food Technology, Slovak University of Technology in Bratislava, Radlinského 9, 812 37 Bratislava, Slovakia
* Correspondence: n.sorokova@ukr.net

Abstract: An important process in the technology of plant oil production by mechanical pressing is the wet–heat treatment of crushed oilseeds, in which the oilseed (compressed seed) is exposed to saturated vapor and a conductive heat supply. Optimal mode selection of wet–heat treatment based on a detailed study of the physical processes taking place in the compressed seed increases oil release, improves its quality indicators, and decreases energy consumption. Mathematical modeling is an advanced method for studying the dynamics of humidification and frying in the compressed seed. The article introduces a mathematical model and a numerical method for calculating heat-and-mass transformation and phase conversion in the process of the humidification and frying of compressed seeds of the castor plant in a continuous multi-stage heating kettle. This study provides equations for calculating the intensity of phase transformation on the inner and outer surfaces of the wet layer. Data verification indicates the adequacy of the mathematical model, effectiveness of the numerical method, and possibility of their use in optimizing the modes of wet–heat treatment for compressed seed raw material.

Keywords: compressed seed humidification; frying; diffusion and filtration transfer; evaporation; condensation

Citation: Sorokova, N.; Didur, V.; Variny, M. Mathematical Modeling of Heat and Mass Transfer during Moisture–Heat Treatment of Castor Beans to Improve the Quality of Vegetable Oil. *Agriculture* **2022**, *12*, 1356. https://doi.org/10.3390/agriculture12091356

Academic Editor: Joanna Miedzianka

Received: 9 August 2022
Accepted: 29 August 2022
Published: 1 September 2022

1. Introduction

Castor plant seeds contain around 50–55% of castor oil, which contains approximately 90% of ricinoleic acid glycerides that are not found in oils of other plants. Due to its chemical and physical properties, especially its weakly temperature-dependent high viscosity, and relative inertness, the oil of the castor plant is widely used in the military, chemical, mechanical, radio electronic, electrical, paint and varnish, medical, cosmetic, and other industries.

Using mechanical pressing or solvent extraction enables plant oil to be obtained from the crushed seed mass. The first method gives a lower oil yield but it has a number of advantages, including lower equipment costs and higher oil quality [1].

The most essential process in the technology of plant oil production by the mechanical method is wet frying of crushed oilseed. There are two stages in the frying process. The first stage represents the heating and wetting of crushed seeds with water or vapor to optimal conditions that are necessary for further seed processing. During the second stage, the wet compressed seed is dried using a power supply and additionally heated. Under such wet–heat treatment, the optimal compressed seed structure for further pressing is created, allowing for increased oil yields. Furthermore, the oil changes its physical properties, with

a decrease in viscosity, density, and boundary tension, and improvement in its quality indicators [2].

The process of compressed seed frying takes place in a continuous multi-stage heating kettle (Figure 1).

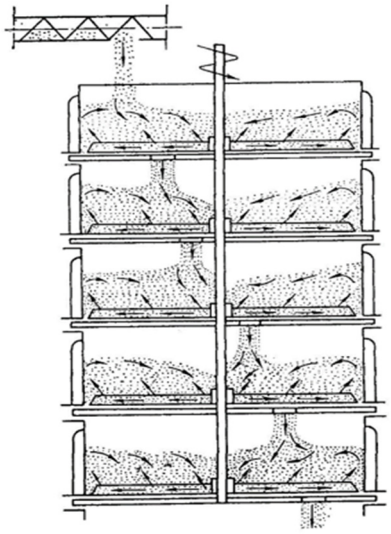

Figure 1. Scheme of continuous multi-stage heating kettle.

The vats have a cylindrical configuration and there are turbine agitators with inclined blades at the heating bottoms. High-pressure saturated vapor is supplied to the bottom of the vats to the internal cavities. The temperature of the vats' side walls under the regular operation mode of the brazier, and the given efficiency of external thermal isolation, is set equal to the temperature of the bottom. Compressed seed is fed into the first vat, where the bottom and side surfaces are heated and wet saturated vapor is supplied to the upper surface of the layer. Then, humid raw material is fed into the second and following vats, where it is fried and dried due to the heat supply. The residence time of the compressed seed in each vat is the same. Turbine mixers rotate and continuously transfer particles within the layer to protect the raw oil material from overheating. The particles move in the radial and vertical direction [3], which increases the thickness of the dispersed wet layer. The frequency of turbine mixers' rotation determines the contact time of the compressed seed with the heated surfaces of the vat bottom.

Seeds of the castor plant belong to the class of colloidal capillary–porous materials. In the process of their grinding, a significant part of the oil is released and adsorbed by the surfaces of the particles. Compressed seed consists of particles of uniform size, with a diameter of 1 mm, and represents a dispersed system, with their structure characterized by the porosity of the P particles and the ε_{la} layer. The spaces between particles are called transport pores [4] and they are partially filled with water, oil, vapor, and air. Oil consists of nonpolar molecules, which is why there are no chemical bonds between its molecules and water molecules. The mass content of solid and oil phases remains unchanged.

During compressed seed processing by saturated vapor, the vapor condenses on the surfaces of the dispersed layer, fills the transport pores, and is adsorbed by the particles. Uniform distribution of the components of the bound substance over the volume of the dispersed layer can thus be assumed. Mass transfer in the system occurs both in the liquid and vapor phases, as well as in air.

The modes of wet–heat treatment of compressed castor seed are determined by the regularities of the processes of heat and mass transfer and phase transformations in the processes of adsorption and desorption in the porous system. An experimental study of the kinetics of these processes in each vat represents a technically complicated and costly task. An attempt to describe the kinetics and dynamics of compressed seed dehydration is re-

stricted by semi-empirical research methods based on balance equations or a mathematical model using Fick's equation for drying (A.V. Lykov [5]).

Paper [6] proposes a mathematical model of the drying kinetics of a dispersed layer of wheat seeds, which was used in [7] to describe oilseed drying (flax, rapeseed, etc.) in "heating–cooling" modes. One of the simplifying assumptions is the linear dependence of the average material temperature on its humidity. The model includes three equations: an equation of the kinetics of heating wet products in oscillating modes [8] to calculate the average temperature T of the material, and differential equations of the heat and material balances to calculate temperature $T_{d.a.}$ of the drying agent and the bulk density of the dispersed layer. The system of equations considers a number of specific coefficients and the average humidity W of the material. For their determination, it is necessary to conduct an experiment. This approach is not universal as the empirical information changes for each drying mode. In addition, the thermophysical parameters of the material, considered to be constant in the presented papers, significantly vary depending on both W and T.

In paper [9], Fick's differential diffusion equation is used for the mathematical modeling of the convective drying of corn grains. The material was preprocessed using the Controlled Sudden Decompression [10] method, leading to an increase in pores in the corn kernels. However, after such treatment, diffusion mass transfer in the pores is accompanied by filtration and moisture evaporation, which was not taken into account in the mathematical model.

Study [11] gives a mathematical description of pumpkin pulp drying in a fluidized bed, where the required value is the apparatus productivity of the dry product per unit volume V of the drying chamber per unit time P. Based on an experimental study of the drying kinetics, it is possible to calculate the dependence $\Pi\ (W, T, V)$ and the empirical equation for the drying rate dW/dt, the accuracy of which is quite low. Paper [4] presents a mathematical model to calculate the dynamics of temperature distribution during drying of the dispersed layer of vegetable raw material.

Paper [12] shows a mathematical description of compressed seed drying using a mathematical model by A.V. Lykov. This model contains two differential equations: energy and humidity transfer for the porous system as a whole. The weak point of the model is the method of finding the intensity of phase transition. In the mass transfer equation, it is omitted, but in the energy equation, it is taken into account within the phase transition coefficient, which is defined as the ratio of the change in the humidity due to the phase transformation of liquid into vapor to the total change in the humidity as a result of humidity transfer and evaporation. In physical terms, these processes can proceed almost independently, so this method presents the replacement of one required function with another one. To define the phase transition coefficient, it is necessary to conduct experimental studies, though it has been already determined for a number of materials [13]. In [14], a mathematical model of heat and mass transfer in dispersed plant material in the process of drying and heating by an ultra-high-frequency electromagnetic field is presented. It is also based on the model of A.V. Lykov for the diffusion–filtration transfer mechanism, which is supplemented by the differential equation of filtration. This equation, as with the energy equation, contains a phase transformation coefficient. Equations are solved analytically under a number of assumptions. To calculate the process of extraction of target components from oilseeds [15], the mathematical model by A.V. Lykov can be used.

For the mathematical modeling of the process of convective drying of wood in [16], the following equations are involved: equations of molecular energy transfer, Stefan–Maxwell equations for the vapor and air phases, which take into account the influence of the porous structure, and the Darcy filtration equation for the system as a whole. The mathematical model considers also the anisotropic nature of the thermal conductivity of wood, the dependence of heat capacity on vapor content, and the movement of the evaporation zone in the volume of the plate. It has a numerical implementation. From the equation of wet and heat transfer [17], a mathematical model of the drying kinetics in a thin dispersed layer was developed, including the radiative–convective energy supply. In [18], the above

equations are solved analytically using an empirical approach and taking into account material shrinkage. In [19], an approach is presented for the mathematical description of the processes of heat and mass transfer during the frying of vegetable foods in oil, using the equations of energy transfer, momentum, and the mass of the liquid and vapor phases. In [20], hybrid mixture theory (HMT)-based two-scale equations were solved using the finite element method to simulate transport processes during the frying of rice crackers. The model was used to predict the moisture and oil content, pore pressures, evaporation rates, elasticity coefficient, and temperature distribution as a function of frying time and spatial coordinates inside a rice cracker.

Numerical implementation of these approaches requires a significant amount of experimental data to determine the thermophysical parameters of the material and mass transfer characteristics. Moreover, the accuracy of mathematical modeling is significantly reduced if the equations of the energy and mass transfer [14,17,18] are solved independently, and the thermophysical characteristics of the material in the process of frying are considered constant.

To describe the adsorption processes, the system of heat and mass transfer equations containing two basic equations—heat transfer and moisture transfer with a source of sorbed substance—was used [21,22]. The character of mass sources [21–25] was determined by approximate empirical correlation, $\partial W/\partial t = fl_W(W_{eq} - W)$, where the following symbols apply: W_{eq}—equilibrium specific mass content; W—specific mass content. This correlation does not include the influence of the volume density of the absorbent (vapor of the absorbed substance) U_v, which is the function of coordinates and time and allows the transfer of adsorption ($\partial W/\partial t > 0$), where $U_v = 0$, which is physically impossible.

The second stage of the process of the wet and heat treatment of compressed seeds is the steaming of the dispersed layer with a gradual decrease in the humidity and an increase in temperature. Thus, the dehydration of particles located near the heating surfaces of the vats and the humidification of less heated particles located inside the volume of the dispersed layer occur due to the steam condensation on the vats' surfaces. To obtain the correct solution of such a problem, it is necessary to determine the dynamics of the intensity of phase transformations on the outer and inner surfaces of the dispersed layer. In addition, transfer of the liquid and vapor phases in the porous material proceeds independently; therefore, the system of the mass transfer equations must include the mass transfer equations of liquid, vapor, and air. During the heat treatment of thermolabile materials, also of compressed seed, it is important that the temperature of the material does not exceed the maximum permissible value. The most critical in such a relation are the boundary surfaces that are in contact with the source of thermal energy. The possibility to calculate the dynamics of temperature distribution in the material allows the selection of such modes of thermal exposure that can help in preventing the deterioration of the final product quality. Based on the new molecular radiation theory of heat and mass transfer, physically justified expressions of the mass transfer characteristics were obtained in [26]. They enabled the development of closed mathematical models of the dynamics of heat and mass transfer and phase transformation in the processes of drying and adsorption in porous systems.

In this paper, a mathematical model of the dynamics of a full cycle of wet and heat treatment of oilseed raw material in a continuous multi-stage heating kettle is presented, taking into account all the features of the process. The model includes the energy equation written for the system as a whole, and mass transfer equations for liquid, vapor, and air phases in a dispersed layer of porous compressed seed particles. When the layer is moistened, the vapor phase passes into the liquid phase, and when the layer is roasted, the liquid phase passes into the vapor phase. This is reflected in the sign of the source term. Thermophysical characteristics of the dispersed layer are determined considering the changing concentration of the components of the bound substance and the porosity εla of the layer and Π of the porous particles. This mathematical model, in combination with the developed numerical method for its calculation, is a universal method of mathemat-

ical modeling for studying the dynamics of heat and mass transfer processes and phase transformations occurring in a multi-stage cylindrical heating kettle during the wet–heat treatment of crushed castor and other oilseeds. Such studies underlie the effective hardware organization of the moisture–heat treatment of oilseeds in accordance with the required temperature and moisture content of compressed seeds, as well as the design features of the fryer.

2. Materials and Methods

2.1. Mathematical Model

A mathematical model was developed based on the obtained differential Equation (1) of substance transfer W (mass, energy, momentum) introduced in [26] for the deformable bodies:

$$\frac{\partial W}{\partial t} = -\mathrm{div}\mathbf{j}_W + I_W - \frac{W}{1+\varepsilon_V}\frac{\partial \varepsilon_V}{\partial t} \quad (1)$$

Here, t—time; $\mathbf{j}_W$—substance fluence rate W; I_W—power of internal sources of the substance; ε_V—relative volumetric deformation of the body as a result of substance transfer W. In the case of the absence of shrinkable phenomena, relative volumetric deformation $\varepsilon_V = 0$ and (1) transforms into the Umov transport equation.

When the compressed seed is humidified, saturated vapor enters into transport pores, condenses on the outer surface of the particles, and the condensate is partially adsorbed by porous particles. During frying, humidified compressed seed in a thick dispersed layer, under the conditions of a predominantly conductive energy supply, implies its self-vaporizing. In this case, the temperature and moisture content in the layer change relatively slowly and insignificantly, allowing us to neglect the effect of shrinkage on the processes of heat and mass transfer, assuming $\varepsilon_V = 0$.

Transfer of the substance W is carried out by diffusion and filtration: $\mathbf{j}_W = \mathbf{j}_W^{\mathrm{d}} + \mathbf{j}_W^{\mathrm{f}}$. The diffusion current density $\mathbf{j}_\psi^{\mathrm{d}}$ masses of the components of the bound substance (liquids ψ = fl, vapor ψ = v, air ψ = ai) are proportional to the change in the volume component concentration U_ψ and temperature T: $\mathbf{j}_\psi^{\mathrm{d}} = -D_\psi(\nabla U_\psi + \delta_\psi^T \nabla T)$, where D_ψ and δ_ψ^T are the diffusion and relative thermal diffusion coefficients of component ψ. The density of molecular energy flux is proportional to the temperature change and volumetric component concentration ψ of the transferred substance: $\mathbf{j}^{\mathrm{d}} = -\lambda\nabla T + \sum\limits_{\psi} h_\psi \mathbf{j}_\psi^{\mathrm{d}}$, where h_ψ—specific enthalpy of component ψ. Terms that take into account the cross effects of heat and mass transfer can be neglected [26]. Densities of the filtration flow of components of the bound substances are presented as follows: $\mathbf{j}_{\mathrm{fl}}^{\mathrm{f}} = U_{\mathrm{fl}}\mathbf{w}_{\mathrm{fl}}$, $\mathbf{j}_{\mathrm{v}}^{\mathrm{f}} = U_{\mathrm{v}}\mathbf{w}_{\mathrm{g}}$, $\mathbf{j}_{\mathrm{ai}}^{\mathrm{f}} = U_{\mathrm{ai}}\mathbf{w}_{\mathrm{g}}$, where $\mathbf{w_{fl}}$ and $\mathbf{w_g}$ are vector sums of the linear velocity w_l of compressed seed particles in regard to the apparatus body and the speed of the filtration transfer of liquid, $\mathbf{w_{fl}}$, or gas, $\mathbf{w_g}$, phases.

Under the specified conditions of heat supply, the mathematical model of heat and mass transfer and phase transformation in the humidification and frying of a dispersed layer of compressed seed in each vat is described by the following Equations (2) to (5):

$$c_{\mathrm{ef}}\left(\frac{\partial T}{\partial t} + \frac{\partial (w_{\mathrm{ef}\,r}T)}{\partial r} + \frac{\partial (w_{\mathrm{ef}\,y}T)}{\partial y}\right) = \frac{1}{r}\frac{\partial}{\partial r}\left(\lambda_{\mathrm{ef}} r \frac{\partial T}{\partial r}\right) + \frac{\partial}{\partial y}\left(\lambda_{\mathrm{ef}}\frac{\partial T}{\partial y}\right) \pm LI_V \quad (2)$$

$$\frac{\partial U_{\mathrm{fl}}}{\partial t} + \frac{\partial (w_{\mathrm{fl}\,r}U_{\mathrm{fl}})}{\partial r} + \frac{\partial (w_{\mathrm{fl}\,y}U_{\mathrm{fl}})}{\partial y} = \frac{1}{r}\frac{\partial}{\partial r}\left(D_{\mathrm{fl}} r \frac{\partial U_{\mathrm{fl}}}{\partial r}\right) + \frac{\partial}{\partial y}\left(D_{\mathrm{fl}}\frac{\partial U_{\mathrm{fl}}}{\partial y}\right) \pm I_V \quad (3)$$

$$\frac{\partial U_{\mathrm{v}}}{\partial t} + \frac{\partial (w_{\mathrm{g}\,r}U_{\mathrm{v}})}{\partial r} + \frac{\partial (w_{\mathrm{g}\,y}U_{\mathrm{v}})}{\partial y} = \frac{1}{r}\frac{\partial}{\partial r}\left(D_{\mathrm{v}} r \frac{\partial U_{\mathrm{v}}}{\partial r}\right) + \frac{\partial}{\partial y}\left(D_{\mathrm{v}}\frac{\partial U_{\mathrm{v}}}{\partial y}\right) \mp I_V \quad (4)$$

$$\frac{\partial U_{\mathrm{ai}}}{\partial t} + \frac{\partial (w_{\mathrm{g}\,r}U_{\mathrm{ai}})}{\partial r} + \frac{\partial (w_{\mathrm{g}\,y}U_{\mathrm{ai}})}{\partial y} = \frac{1}{r}\frac{\partial}{\partial r}\left(D_{\mathrm{ai}} r \frac{\partial U_{\mathrm{ai}}}{\partial r}\right) + \frac{\partial}{\partial y}\left(D_{\mathrm{ai}}\frac{\partial U_{\mathrm{ai}}}{\partial y}\right) \quad (5)$$

The effective ranges of volume-specific heat capacity c_{ef} and heat conduction λ_{ef} of the compressed seed layer are calculated in the process of wet–heat treatment due to the ratio: $c_{ef} = c_b\rho_b\Psi_b + c_{fl}U_{fl} + c_vU_v + c_{ai}U_{ai}$, $\lambda_{ef} = \lambda_b\Psi_b + \lambda_{fl}U_{fl}/\rho_{fl} + \lambda_vU_v/\rho_v + \lambda_{ai}U_{ai}/\rho_{ai}$, where c_b, c_{fl}, c_v, c_{ai} and λ_b, λ_{fl}, λ_v, λ_{ai}—mass-specific heat capacity and thermal conductivity of dry greasy substance, liquid, vapor, and air; Ψ_b—volume ratio of hard and greasy phase in dispersed layer, $\Psi_b = (1 - \Pi)(1 - \varepsilon_{la})$; L—latent heat of phase transformations; w_{efk}—effective velocity of components' filtration, $w_{ef\,k} = \left[w_{flk}\,c_{fl}U_{fl} + w_{gk}\,(c_vU_v + c_{ai}U_{ai})\right]/c_{ef}$, k ($k = y, r$). By analogy with a fluidized bed, for which the hydrodynamic characteristics are the porosity of the fixed bed and that of the suspended bed [13], the speed of the material and components ψ (ψ = fl, v, ai) of the bound substance in regard to the vat body in the mathematical model depends on the correlation between the change in the dispersed layer thickness, mixers' speed rate [2], and the particular value of layer porosity ε_{la}.

Equation (6), obtained by N.I. Nikitenko [27], can be used to calculate the diffusion coefficient of the liquid phase D_{fl},

$$D_{fl} = \gamma_{Dfl}\left[\exp\left(\frac{A_D}{R_uT}\right) - 1\right]^{-1} \quad (6)$$

Equation (7) shows the vapor and air diffusion coefficients [13,28]:

$$D_v = D_{ai} = \gamma_{Dv}\frac{T^{3/2}}{P_g} \quad (7)$$

where γ_{Dfl} and γ_{Dv} are diffusion coefficients considering the transfer of the substance in the capillaries of particles and transport pores of the layer; A_D is the activation energy of the diffusion process; R_u is the universal gas constant; P_g is the pressure of the gas phase in the porous body.

It should be noted that Equation (6) for D_{fl} transforms into the Arrhenius equation in limit conditions (if $A_D/(R_uT) >> 1$) for solids and into the Einstein equation (if $A_D/(R_uT) << 1$) for liquid media.

Darcy's equation represents the filtration rates of liquid and gas: $w_\psi = -K_0K_\psi/\eta_\psi\nabla P_\psi$ (ψ = fl, g), where K_0 is the total permeability of the medium, K_ψ is the relative permeability, and η_ψ is the dynamic viscosity coefficient. Pressures P_{fl} and P_g are calculated through the required functions U_{fl}, U_v, U_{ai} and T: the volume ratio of the liquid phase in the porous body $\Psi_{fl} = U_{fl}/\rho_{fl}$, gas mixture $\Psi_g = 1 - \Psi_b - \Psi_{fl}$; partial density of vapor and air $\rho_v = U_v/\Psi_g$ and $\rho_{ai} = U_{ai}/\Psi_g$; partial pressures $P_v = \rho_vR_uT/\mu_v$ and $P_{ai} = \rho_{ai}R_uT/\mu_{ai}$, where μ_v and μ_{ai} are the molar masses of vapor and air. Thus, gas phase pressure $P_g = P_v + P_{ai}$, and liquid phase pressure $P_{fl} = P_g + P_{cap}$, where capillary pressure P_{cap} is as the average capillary pressure of the liquid in the body pores [29] (Equation (8)):

$$P_{cap} = 2\sigma(T)\int_{r_{min}}^{r_{max}}\frac{\theta}{r}f(r)dr\Big/\int_{r_{min}}^{r_{max}}\theta f(r)dr = \frac{2\sigma(T)}{r*} \quad (8)$$

where r_{min}, r_{max}—minimum and maximum pore radius; r*—characteristic parameter of pore size dispersion, $r_{min} < r^* < r_{max}$; $f(r)$—differential function of pore distribution according to size; $\theta(r,t) = 1 - (1 - \delta/r)^2$—volume ratio of the liquid in capillaries of radius r at moment t; δ—thickness of the condensate layer.

N.I. Nikitenko [30] derived the equation $\delta = \delta * \bar{\delta} = \delta*(1 - \sqrt{1 - P_v/P_s}) = \delta * (1 - \sqrt{1 - \varphi})$ to define the equilibrium thickness of the condensate layer forming on a solid surface in a gaseous environment with relative humidity φ. Here, δ*—thickness of the condensate layer in which evaporation occurs (determined by the average jump distance of the activated particle of the layer); $\bar{\delta} = \delta/\delta*$ for each layer ($0 < \delta < \delta$*) and $\bar{\delta} = 1$ for a massive layer ($\delta > \delta$*).

The sorption and desorption dynamics of molecules are characterized by two competing processes: the condensation of vapor molecules on the surface of the adsorbing layer, and the evaporation of liquid molecules located next to the free surface of the condensed layer that reached the activation energy. N.I. Nikitenko [30] obtained Equation (9) for the intensity of the phase transformation on the outer surface of the liquid layer:

$$I = \gamma_c \left\{ \varphi_b \left(\exp\left[\frac{A}{R_u T|_{\nu=0}} \right] - 1 \right)^{-1} - \varphi_{e.m.} \left(\exp\left[\frac{A}{R_u T_{e.m.}} \right] - 1 \right)^{-1} \right\}, \; \gamma_c = \frac{\varepsilon \rho_{fl} \delta *}{4}, \tag{9}$$

This equation was used to calculate the intensity of phase transformation on the outer surface of the liquid layer of the compressed castor seed. Here, γ_c—coefficient of surface evaporation; ε—emission coefficient; A—activation energy; φ_b—humidity of the body, which, due to the sorption isotherm, is equal to the humidity of the vapor and gas mixture and correlates with the liquid concentration U_{fl} in this point of the porous body; ν—standard boundary surface; $T_{e.m.}$ and $\varphi_{e.m.}$—temperature and relative humidity of the environment.

The term member within the curly brackets in Equation (9) shows the intensity of the evaporation rate, while the second represents the intensity of the sorbent condensation. If the first term is higher than the second one, liquid desorption is considered; otherwise, the adsorption process takes place.

N.I. Nikitenko [30] used equation $P_s = N_P \sqrt{T} [\exp(A/R_u T) - 1]^{-1}$ to calculate the saturation pressure P_s; if N_P = const., it shows good correlation with tabulated data. In the temperature range $0 \leq T \leq 100$ °C, where $N_P = 0.4361 \times 10^{10}$ kg/(m·s^2·K$^{0.5}$), the maximum error of calculation deviation from the tabulated data P_s is 3.4%.

The specific intensity of phase transformation in the compressed seed layer is defined by Equation (10), which follows from Equation (9) under the condition of local thermodynamic equilibrium of the contacting phases:

$$I_V = \gamma_V \left[\exp\left(\frac{A}{R_u T} \right) - 1 \right]^{-1} (\varphi_b - \varphi), \tag{10}$$

where γ_V—coefficient of volumetric evaporation, and $\gamma_V = \gamma_c S$, φ—relative humidity of vapor and gas mixture in the pores of the porous layer. To determine the contact surface area S of the liquid and gas phases in the partially filled pores of a unit volume of the porous body [26,28], the following Equation (11) is used:

$$S = \frac{2\sqrt{1 - \varphi_b}}{\rho_{fl} \delta *} \frac{\partial U_{fl}}{\partial \varphi_b}. \tag{11}$$

The derivative $\partial U_{fl} / \partial \varphi_b$ is determined from the desorption isotherm equation. Data [30] on the equilibrium humidity of compressed seed raw material W_{eq} are quite well approximated by the equation $W_{eq} = 20.3\varphi_b{}^3 - 3.2\varphi_b{}^2 + 3.03$. Transition to volume density was carried out due to the equation $U_{fl} = 0.01\, W \rho_b$.

2.2. Single-Value Condition

It is necessary to set the initial and boundary conditions to solve the system of Equations (2)–(5). At the beginning of the humidification process of compressed castor seed, the temperature $T(r,y,0)$ and concentration of the bound substance components $U_{fl}(r,y,0)$, $U_v(r,y,0)$, $U_{ai}(r,y,0)$ are assumed to be the same at all points of the dispersed layer. Initial values of the required functions in each following vat of the brazier are expected to be equal to their average values after compressed seed processing in the previous vat.

Boundary conditions of heat and mass transfer are set for each surface of the computational domain (Figure 2), bound by the lower and side walls of the vat, the surface of the turbine agitator shaft, and the layer of vapor and gas mixture.

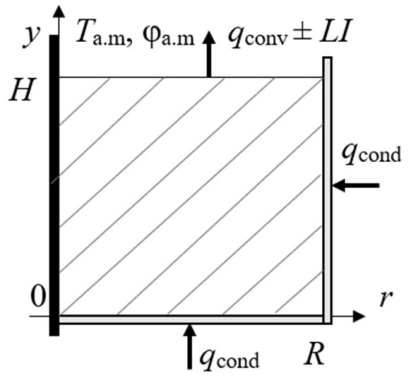

Figure 2. View of the computational domain.

On the surface, $y = H$, $0 \le r \le R$; in the first stage of compressed seed humidification, wet vapor is supplied; in the process of frying, water is evaporated.

These processes describe the boundary conditions of the third kind, as in Equations (12) to (15):

$$\lambda_{ef} \frac{\partial T}{\partial y}\bigg|_{y=H} = \mp\alpha(T|_{y=H} - T_{e.m.}) \pm L\,I|_{y=H} \tag{12}$$

$$D_{fl} \frac{\partial U_{fl}}{\partial y}\bigg|_{y=H} + \frac{\partial (w_{fl\,y} U_{fl})}{\partial y}\bigg|_{y=H} = \pm I|_{y=H} \tag{13}$$

$$D_v \frac{\partial U_v}{\partial y}\bigg|_{y=H} + \frac{\partial (w_{vy} U_v)}{\partial y}\bigg|_{y=H} = \mp\gamma_{v,e.m.} \left(U_v|_{y=H} - \rho_{v,e.m.}\psi_v \right) \tag{14}$$

$$U_{ai}|_{y=H} = \frac{P_{e.m.}\psi_g \mu_{ai}}{R\,T|_{y=H}} - U_{ai}|_{y=H} \frac{\mu_{ai}}{\mu_v} \tag{15}$$

Expression (14) is obtained from [26,29] considering the following conditions: when the system enters the equilibrium state $t \to \infty$, parameters $\rho_v = \rho_{va.m.}$, $T|_{y=H} = T_{e.m.}$.

On the boundary, $0 \le y \le H$, $r = 0$, of the computational domain, the conditions for the symmetry of the field of the desired functions are set, as in Equation (16):

$$\frac{\partial T}{\partial r}\bigg|_{r=0} = 0;\ \frac{\partial U_{fl}}{\partial r}\bigg|_{r=0} = 0;\ \frac{\partial U_v}{\partial r}\bigg|_{r=0} = 0;\ \frac{\partial U_{ai}}{\partial r}\bigg|_{r=0} = 0;\ \frac{\partial w_{flr}}{\partial r}\bigg|_{r=0} = 0;\ \frac{\partial w_{gr}}{\partial r}\bigg|_{r=0} = 0. \tag{16}$$

On the right ($0 \le y \le H$, $r = R$) and lower ($y = 0$, $0 \le r \le R$) boundaries that are in contact with the heated surfaces of vats, heat transfer conditions of the fourth kind are set, and mass transfer is absent, as in Equations (17) and (18):

$$\lambda_{wall} \frac{\partial T_1}{\partial \delta_{wall}}\bigg|_{r=R} = \lambda_{ef} \frac{\partial T}{\partial r}\bigg|_{r=R};\ T_1|_{r=R} = T|_{r=R} + \Delta T;\ \frac{\partial U_{fl}}{\partial r}\bigg|_{r=R} = 0;\ \frac{\partial U_v}{\partial r}\bigg|_{r=R} = 0;\ \frac{\partial U_{ai}}{\partial r}\bigg|_{r=R} = 0; \tag{17}$$

$$\lambda_{wall} \frac{\partial T_{wall}}{\partial \delta_{wall}}\bigg|_{y=0} = \lambda_{ef} \frac{\partial T}{\partial y}\bigg|_{y=0};\ T_{wall}|_{y=0} = T|_{y=0} + \Delta T;\ \frac{\partial U_{fl}}{\partial y}\bigg|_{y=0} = 0;\ \frac{\partial U_v}{\partial y}\bigg|_{y=0} = 0;\ \frac{\partial U_{ai}}{\partial y}\bigg|_{y=0} = 0. \tag{18}$$

Temperature difference ΔT between the wall and compressed seed occurs due to the vapor and gas layer formation as a result of turbine mixer operation to prevent material overheating, $\Delta T = q_{in}\delta_{in}/\lambda_{g\,in}$, where δ_{in}/λ_g—thermal resistance of the interlayer, q_{in}—heat transfer density through the interlayer.

2.3. Numerical Method of Solution

The system of differential Equations (2)–(5) is essentially non-linear. Its implementation is possible only using a numerical method. Equations (2)–(5) contain diffuse and convective terms, and to solve them, implicit difference schemes are usually used. Their main advantage is the stability of the obtained solution; however, the complexity of solving even one-dimensional linear differential equations is a significant disadvantage. Based on the method of combining difference schemes, N.I. Nikitenko [26] obtained an explicit three-layer recalculation difference scheme consisting of a combination of explicit and implicit schemes, multiplied by weight factors and added up. The most famous scheme for solving differential equations of the parabolic type is the absolutely stable Crank–Nicolson scheme. The indicated explicit three-layer recalculation difference scheme was developed to solve convective transfer equations by combining difference transfer equations in the explicit form for time layer t_n and in the implicit form for time layers t_{n-1} and t_{n-2}, respectively, and for the splitting procedure [26]. This scheme is characterized by the simplicity of explicit schemes and, as with the known implicit schemes, it allows the selection of the steps of the difference grid arbitrarily. In cylindrical coordinates on proportional difference mesh $r_i = (i-1)\,h$, $(i = 1,\ldots, IK;\ h = \text{const})$, $y_m = (m-1)\,h_y$, $(m = 1,\ldots, MK;\ h_y = \text{const})$, $t_n = nl$ $(n = 0,1,\ldots, l > 0)$, where h, h_y and l are steps of the difference mesh, each differential equation is approximated by two finite difference equations: the first takes into account the change in the required function as a result of filtration substance transfer, and the second one considers the change due to diffusion, filtration, and phase transformations. The energy transfer Equation (2), in accordance with the mentioned scheme, is presented in the form of Equations (19) and (20):

$$\begin{aligned}\frac{\overline{T}_{i,m}^{n+1}-T_{i,m}^{n}}{l} &= -\left[\left((w_{\text{efr}}T)_{i+1,m}^{n}-(w_{\text{efr}}T)_{i,m}^{n}\right)-\left((w_{\text{efr}}T)_{i,m}^{n}-(w_{\text{efr}}T)_{i-1,m}^{n}\right)\right]/\left(2h^2\right)\\ &-\left[\left((w_{\text{efy}}T)_{i,m+1}^{n}-(w_{\text{efy}}T)_{i,m}^{n}\right)-\left((w_{\text{efy}}T)_{i,m}^{n}-(w_{\text{efy}}T)_{i,m-1}^{n}\right)\right]/\left(2h_y^2\right),\end{aligned} \tag{19}$$

$$\begin{aligned}(1+\Omega_T)\frac{T_{i,m}^{n+1}-\overline{T}_{i,m}^{n+1}}{l}-\Omega_T\frac{T_{i,m}^{n}-T_{i,m}^{n-1}}{l} &= -\left[\left((w_{\text{efr}}\overline{T})_{i+1,m}^{n+1}-(w_{\text{efr}}\overline{T})_{i,m}^{n+1}\right)-\right.\\ \left.\left((w_{\text{efr}}\overline{T})_{i,m}^{n+1}-(w_{\text{efr}}\overline{T})_{i-1,m}^{n+1}\right)\right]/\left(2h^2\right) &- \left[\left((w_{\text{efy}}\overline{T})_{i,m+1}^{n+1}-(w_{\text{efy}}\overline{T})_{i,m}^{n+1}\right)\right.\\ -\left.\left((w_{\text{efy}}\overline{T})_{i,m}^{n+1}-(w_{\text{efy}}\overline{T})_{i,m-1}^{n+1}\right)\right]/\left(2h_y^2\right) &+ \frac{1}{c_{\text{ef}}}\left\{\frac{1}{2r_{i,m}}\left[\left(\lambda_{\text{ef}i+1,m}r_{i+1,m}+\lambda_{\text{ef}i,m}r_{i,m}\right)\left(\overline{T}_{i+1,m}^{n+1}-\overline{T}_{i,m}^{n+1}\right)\right.\right.\\ -\left.\left(\lambda_{\text{ef}i,m}r_{i,m}+\lambda_{\text{ef}i-1,m}r_{i-1,m}\right)\left(\overline{T}_{i,m}^{n+1}-\overline{T}_{i-1,m}^{n+1}\right)\right]/h^2 &+ \left[\left(\lambda_{\text{ef}i,m+1}+\lambda_{\text{ef}i,m}\right)\left(\overline{T}_{i,m+1}^{n+1}-\overline{T}_{i,m}^{n+1}\right)-\right.\\ \left.\left.\left(\lambda_{\text{ef}i,m}+\lambda_{\text{ef}i,m-1}\right)\left(\overline{T}_{i,m}^{n+1}-\overline{T}_{i,m-1}^{n+1}\right)\right]/\left(2h_y^2\right)-I_V\right\}\end{aligned} \tag{20}$$

Difference approximations of Equations (3)–(5) are written similarly. The weight parameter Ω_T removes the time restrictions in one step, $\Omega_T \geq 0$. The approximation error has the order $l + h^2 + h_y^2$. The necessary condition for the stability of the finite difference equation, obtained based on the method of the conditional task of some required functions of the system [26], is presented in Equation (21):

$$l \leq \left\{\left(\frac{w_r}{h}+\frac{w_y}{h_y}\right)^{-1};\ \frac{(1+2\Omega)}{2\nu\left(h^{-2}+h_y^{-2}\right)}\right\} \tag{21}$$

where w_r and w_y stand for $w_{\text{ef}\,k}$, $w_{\text{fl}\,k}$, $w_{\text{g}\,k}$ $(k = r, y)$; parameter ν is equal to $\lambda_{\text{ef}}/c_{\text{ef}}$, D_{fl}, D_{v}, and D_{ai} for Equations (2)–(5). The calculated time step for solving the equation system (2)–(5) is chosen from the condition $l \leq \min(l_T; l_{\text{fl}}; l_{\text{v}}; l_{\text{ai}})$. After an arbitrary choice of steps of the difference mesh, h, h_y are defined according to (21) by [26] Ω_T, Ω_{fl}, Ω_{v}, Ω_{ai}.

To calculate the temperature at the nodal points $(i, 1)$ at the boundary $y = 0$, $0 \le r \le R$ of the computational domain (Figure 2), instead of Equation (20), the difference approximation is used, including the thermal resistance of the vapor and gas interlayer between the bottom and the wet layer, as in Equation (22):

$$(1+\Omega_{\mathrm{T}})\frac{\tilde{T}_{i,1}^{n+1}-\overline{T}_{i,1}^{n+1}}{l}-\Omega_{\mathrm{T}}\frac{T_{i,1}^{n}-T_{i,1}^{n-1}}{l}=-\left[\left((w_{\mathrm{efr}}\overline{T})_{i+1,1}^{n+1}-(w_{\mathrm{efr}}\overline{T})_{i,1}^{n+1}\right)-\left((w_{\mathrm{efr}}\overline{T})_{i,1}^{n+1}-(w_{\mathrm{efr}}\overline{T})_{i-1,1}^{n+1}\right)\right]/(2h^2)$$
$$-\left[\left((w_{\mathrm{efy}}\overline{T})_{i,2}^{n+1}-(w_{\mathrm{efy}}\overline{T})_{i,1}^{n+1}\right)-\left((w_{\mathrm{efy}}\overline{T})_{i,1}^{n+1}-(w_{\mathrm{efy}}\overline{T})_{i,2}^{n+1}\right)\right]/\left(2h_y^2\right)+\frac{1}{c_{\mathrm{ef}}}\left\{\frac{1}{2r_{i,1}}\left[\left(\lambda_{\mathrm{ef}i+1,1}r_{i+1,1}+\lambda_{\mathrm{ef}i,1}r_{i,1}\right)\left(\overline{T}_{i+1,1}^{n+1}-\overline{T}_{i,1}^{n+1}\right)\right.\right.$$
$$\left.-\frac{1}{h_y/\lambda_{\mathrm{ef}i,1}+\delta_{\mathrm{il}}/\lambda_{\mathrm{g\ il}}}\left(\overline{T}_{i,1}^{n+1}-\overline{T}_{\mathrm{wa}}^{n+1}\right)\right]/(h_y+\delta_{\mathrm{il}})-I_V\Big\} \quad (22)$$
$$-\left(\lambda_{\mathrm{ef}i,1}r_{i,1}+\lambda_{\mathrm{ef}i-1,1}r_{i-1,1}\right)\left(\overline{T}_{i,1}^{n+1}-\overline{T}_{i-1,1}^{n+1}\right)\Big]/h^2+\left[\frac{\left(\lambda_{\mathrm{ef}i,2}+\lambda_{\mathrm{ef}i,1}\right)}{2h_y}\left(\overline{T}_{i,2}^{n+1}-\overline{T}_{i,1}^{n+1}\right)\right.$$
$$\left.-\frac{1}{h_y/\lambda_{\mathrm{ef}i,1}+\delta_{\mathrm{il}}/\lambda_{\mathrm{g\ il}}}\left(\overline{T}_{i,1}^{n+1}-\overline{T}_{\mathrm{wa}}^{n+1}\right)\right]/(h_y+\delta_{\mathrm{il}})-I_V\Big\}$$

The difference equation for the nodal points (I, m) is written similarly to (22).

As a result of system solution (2)–(5), the ranges of temperatures, pressures, and filtration rates, and volumetric concentrations of the liquid, vapor, and air phases in the dispersed layer, are found. Real concentrations of components $U_{\mathrm{fl}}^{\mathrm{true}}$, $U_{\mathrm{v}}^{\mathrm{true}}$, and $U_{\mathrm{ai}}^{\mathrm{true}}$, associated with the compressed seed particles, are calculated from the ratio:

$$U_{\mathrm{fl}}^{\mathrm{true}}=U_{\mathrm{fl}}(1-\varepsilon_{\mathrm{la}}),\ U_{\mathrm{v}}^{\mathrm{true}}=(U_{\mathrm{v}}+\rho_{\mathrm{v}}\varepsilon_{\mathrm{la}}),\ U_{\mathrm{ai}}^{\mathrm{true}}=(U_{\mathrm{ai}}+\rho_{\mathrm{ai}}\varepsilon_{\mathrm{la}}). \quad (23)$$

2.4. Approbation

According to the technological regulations, presented in [2], inactivation of the enzyme system of compressed castor seed starts in a screw inactivator by exposure to saturated vapor for 30–40 s; at the same time, the raw material humidity increases to 9–10% and its temperature rises to 80–83 °C. In the first heating vat of the brazier, the raw material is additionally humidified to the wet content of 13–13.5% and heated to 85 °C. In the following vat, heated and humidified compressed seed is subjected to fry-heat treatment with its gradual heating to the temperature of 100–105 °C, self-vaporizing, and dehydration to wet content of 5–6%.

Based on the developed mathematical model and numerical method, we conducted the calculation of the dynamics and kinetics of the humidification and frying of the compressed castor seed in an experimental seven-vat brazier. Productivity of the brazier was 625 kg/h. The inner diameter of each vat was 1 m, and its estimated capacity was 95 kg; the thickness of the hollow bottoms was 0.01 m. The height of the compressed seed layer in the heating vat in stationary state was h = 0.21 m; the effective layer thickness during mixer rotation was H = 0.5 m. Accordingly, the porosity of the layer was $\varepsilon_{\mathrm{la}} = 1 - \mathrm{h/H} = 0.6$. Physical properties of the solid fatty phase of castor seed [31]: $c_{\mathrm{b}} = 1.915$ kJ/(kg·K); $\lambda_{\mathrm{b}} = 0.15$ W/(m·K); $\rho_{\mathrm{b}} = 1025$ kg/m^{-3}, $\Pi = 0.385$. Activation energy $A = A_D = 0.4205 \times 10^8$ J/kmol. Diffusion coefficients were determined from the solution of the inverse problem: $\gamma_{D\mathrm{fl}} = 0.125 \times 10^{-9}$ m^2/s; $\gamma_{D\mathrm{v}} = 0.34 \times 10^{-5}$ m^2/s.

The problem was solved with initial data presented in Table 1.

The time for the processing of compressed castor seed in each heating vat is approximately 514 s. This was established from the duration of the castor seed moisturizing in the first vat and the duration of its complete roasting in a batch laboratory two-vat brazier with the same geometrical characteristics of the heating vats. When roasting castor seed in the second vat, its moisture content was determined [32] at time intervals $\Delta t = 514$ s based on the material balance equation: $G(W_0 - W) = V_{\mathrm{dr.ai}}(d - d_0)$. Here, G is the consumption of dry fatty matter of the castor plant, kg/s; $V_{\mathrm{dr.ai}}$ is the consumption of dry air in contact with the castor plant, kg/s; W_0, W are the initial and current average moisture content of the material for the time interval Δt, kg/kg of dry material; d_0 and d are the initial and current moisture content of wet air during time Δt, in kg/kg of dry air. According to the known initial

moisture content of castor seed of W_0 = 9.5% and the weight of wet castor seed in the first vat (90 kg), the weight of the liquid was found to be m_{fl0} = 90·0.095 = 8.55 kg and the weight of the dry fatty material was m_b = 81.45 kg. Dry air mass flow $V_{dr.ai} = V_{ai0}/(1 + d_0 \cdot 0.001)$, where V_{ai0}, as the flow rate of exhausted moist air, was determined by a flow meter. Current air moisture content $d_1 = 622\ P_{v\ a.m.}/(P_{a.m.} - P_{v\ a.m.})$ was calculated based on the readings of the psychrometer, which recorded the temperature and relative humidity of air removed from the vat. Then, the current moisture content of the castor seed was $W = W_0 - V_{dr.ai}(d - d_0)/G$. In the first time interval Δt, the initial moisture content was W_0 = 13.5%. The values of W at the end of six identical time intervals Δt were 11.76, 9.6, 8.1, 7.1, 6.5, 6%.

Table 1. Initial data for the compressed castor seed and the environment.

Humidification	Frying
Initial compressed seed parameters:	Initial compressed seed parameters:
T_0 = 80 °C;	T_0 = 85 °C;
W_0 = 9.5%;	W_0 = 13.5%;
U_{l0} = 48.7 kg/m^{-3};	Parameters of vapor and gas mixture:
Wet saturated vapor:	$T_{a.m.}$ = 75 °C;
$T_{a.m.}$ = 101 °C;	$P_{a.m.}$ = 0.1 MPa;
$\varphi_{a.m.}$ = 1;	$P_{v\ a.m.}$ = 2.5 kPa;
Heating vapor, supplied to the bottom of the kettle:	Heating vapor, supplied to the bottom of the vat:
$P_{h..v}$ = 0.5 MPa;	$P_{h..v}$ = 0.5 MPa;
$T_{h..v}$ = 151.8 °C.	$T_{h..v}$ = 151.8 °C.

A spatial grid along with the thickness H and radius R (Figure 2) was built in eight spaces so that the space along the thickness was hy = H/8 and the radius h = R/8. Thus, there were IK = MK = 9 nodal points at each coordinate.

The results of the numerical simulation were obtained using computer programs created in the FORTRAN algorithmic language.

3. Results

Figure 3 shows the average humidity and temperature of the compressed seed during the whole cycle of wet–heat treatment in the seven-vat brazier. The results were obtained by mathematical modeling and calculation [32] of discrete values of average compressed seed humidity after each vat using the balance method. Curves of humidity change are characterized by the moments of constant and the decreasing speed that corresponds to the actual process. In the humidification process, the average compressed seed temperature increases as a result of its contact with hot vat surfaces, wet saturated vapor, and the release of the heat of adsorption. In the frying process, the temperature significantly increases during each pouring into the following vat due to an increase in separate particles of the dispersed layer falling into the contact zone with vat surfaces. Moreover, the compressed seed temperature in the second and third vats slightly decreases at first due to the intensive evaporation of water from the layers that are in contact with the heating surfaces, and then the temperature increases as a result of partial vapor condensation on the raw material particles remote from the heat exchange surfaces.

Gradual equalization of the average temperature of all particles of dispersed layers of compressed seed occurs in the subsequent vats without any vapor condensation. During the heating of the dispersed layer in each vat, the average temperature of the material slightly decreases as a result of the evaporation and direct release of the resulting vapor from the brazier into the environment.

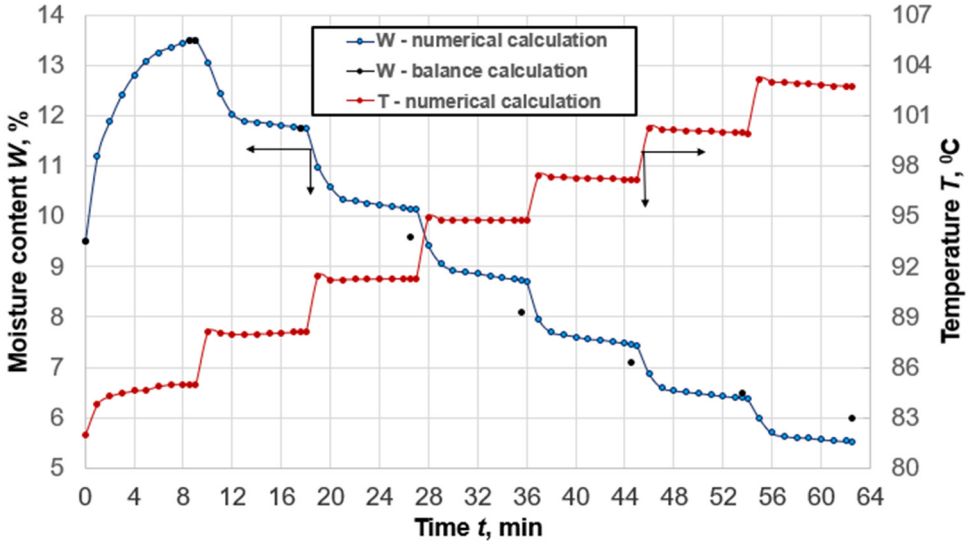

Figure 3. Change in average values of humidity and temperature of compressed castor seed in time in the process of wet–heat treatment in a seven-vat brazier, obtained by mathematical model (lines) and balance calculations (dots).

The average humidity of the compressed seed of the castor plant at the end of each frying process, obtained by numerical and balance calculations, agrees quite well and the discrepancy does not exceed 7%, which indicates the adequacy of the mathematical model and the effectiveness of the numerical method of calculation.

Areas of local temperature values and humidity concentration over the volume of the dispersed compressed seed layer in each vat under the appropriate physical and geometric conditions of uniqueness can be significantly uneven. The results of numerical dynamic modeling of heat and mass transfer in the process of wet and heat transfer of the compressed castor seed improve this result. Figure 4 shows the change in the local values of the liquid volume concentration along the height of the dispersed layer of the compressed castor seed when it is treated with wet vapor at different points in time. It represents the central section along the radius of the first vat.

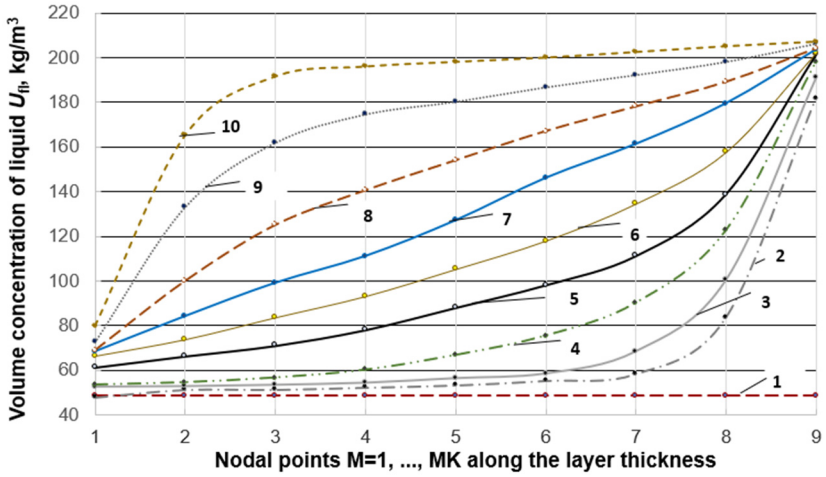

Figure 4. Dynamics of liquid volume concentration U_{fl} change along the height H of the oil dispersed layer at nodal points m (MK = 9) in the cross-section along the radius $r = R/2$ (i = 5) humidified in the first vat: 1—t = 0 min, 2—t = 1 min, 3—t = 2 min, 4—t = 3 min, 5—t = 4 min, 6—t = 5 min, 7—t = 6 min, 8—t = 7 min, 9—t = 8 min, 10—t = 8.57 min.

Saturated vapor is supplied to the first vat and it begins to condense on the outer surfaces of the compressed seed dispersed layer located next to the boundary $y = H$ ($M = 9$), sharply increasing the concentration of the liquid phase in the boundary layers. Then, the vapor, moving along the transport pores, condenses on the particles located further and further from the outer surface. The condensate moves deep into the layer by diffusion and filtration through the transport pores and capillaries of the particles.

Figures 5 and 6 show curves of changes in the liquid volume concentration U_{fl} and temperature change T along the thickness of the oil layer H at each stage of the frying process; particular sections are shown along the vat radius at the time of 8 min, providing an average section of $r = R/2$ and the section next to the hot side surface $r = R$.

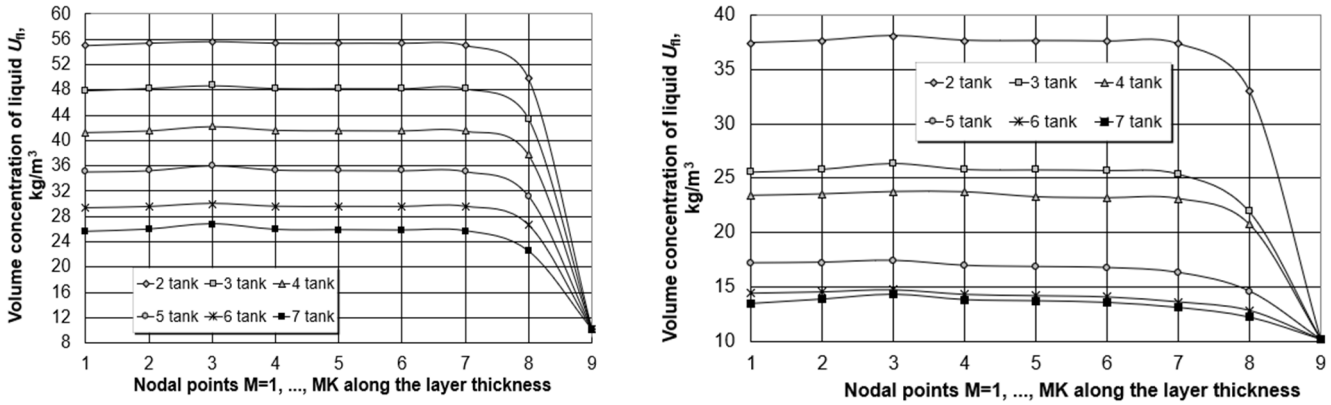

Figure 5. Change in the volume concentration of the liquid phase U_{fl} during compressed castor seed frying along the layer height in sections $r = R/2$ (**a**) and $r = R$ (**b**) in each vat at the time of 8 min.

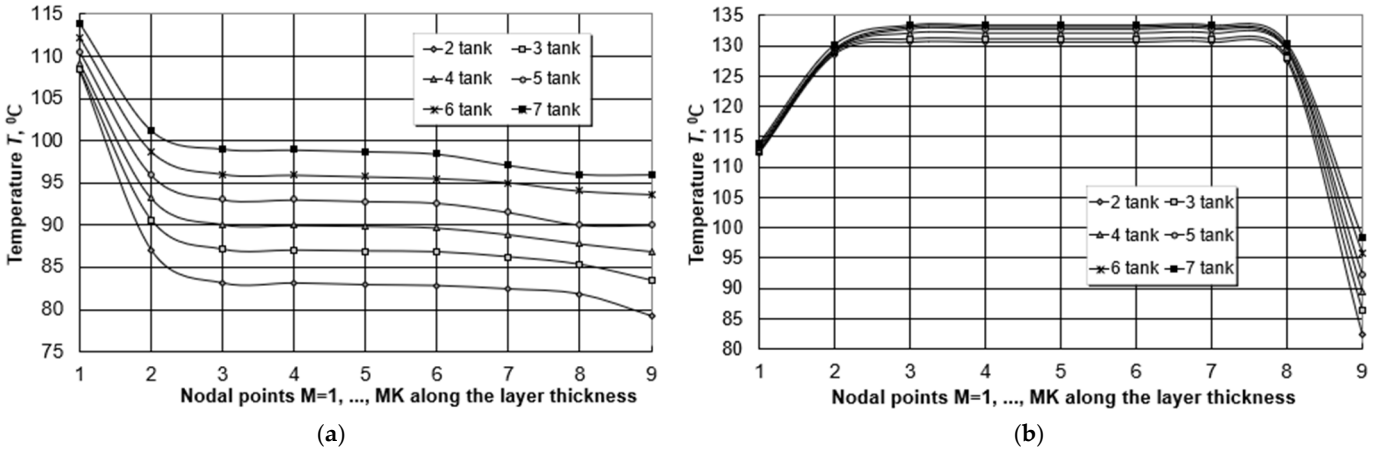

Figure 6. Temperature change T of compressed castor seed in the frying process along the layer height in sections $r = R/2$ (**a**) and $r = R$ (**b**) in each vat at 8 min.

The time point of 8 min corresponds to almost the end of the frying process of the compressed seed in each vat. During the period of drying rate decreasing, the concentration of the liquid phase on the surface of the material that is in contact with the outside gas environment is equal to its equilibrium value [27].

Thus, the volume concentration of the liquid U_{fl} at nodal point 9 corresponds to the equilibrium value at the given temperature $T_{a.m.}$ and relative humidity $\varphi_{a.m.}$ of the gas environment in vats. When the compressed seed is in contact with the hot bottoms of the vats ($M = 1$), its intense dehydration occurs and U_{fl} decreases faster than at the inner points. The formed vapor passes through the dispersed layer, partially condensing, and increases

the concentration U_{fl} of the colder middle interlayers. In each following vat, U_{fl} is lower than in the previous one.

The maximum temperature of the oil raw material is reached in the areas of its contact with the side heating surfaces of vats (b). It exceeds the temperature of the compressed seed at the bottoms of the vats (M = 1) since the blades of the turbine agitator create a gas interlayer between the wet layer and the bottom and prevent thus longer contact with the hot surface.

Thermal resistance of the compressed seed contact with side surfaces of vats will be lower due to the centrifugal force created by the turbine that directs particles located at the bottom in the radial direction, where they reach the side surface as they move upwards. The area next to the side vats' surface is the most critical in terms of retaining the beneficial properties of castor oil.

Depending on the scale of oil production, it is advisable to use devices for the wet–heat processing of oil raw materials with optimal productivity. The productivity of the multi-stage heating kettle can be adjusted by changing the geometric parameters of the vat. The developed mathematical model allows us to describe the roasting process in cylindrical configuration devices of any size, specifying them when building a difference grid. Figure 7 presents the results of mathematical modeling of the kinetics of wet–heat treatment of compressed castor seed in a seven-stage heating kettle, with the vat diameter of 1.58 m, using other initial data as in the previous calculation.

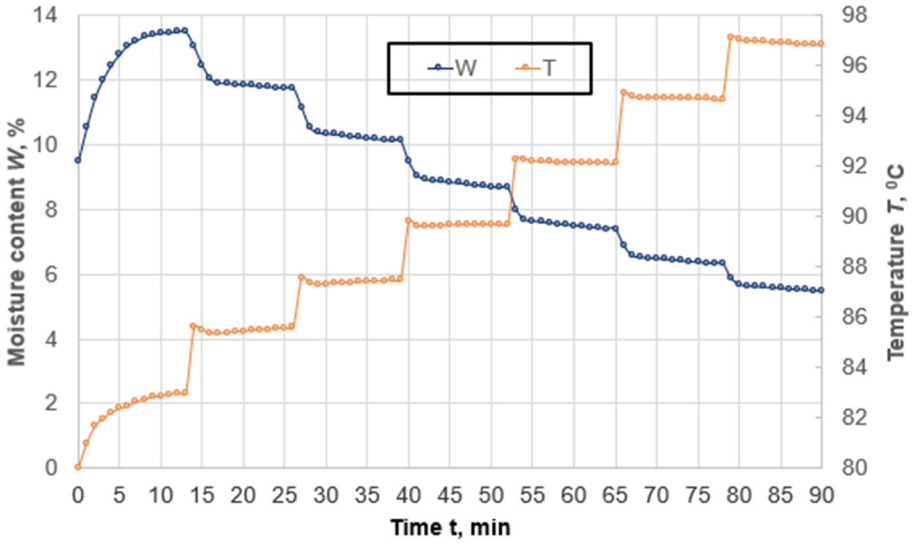

Figure 7. Change in average temperature and moisture content of compressed castor seed in a seven-stage heating kettle with vat bottom diameter of 1.58 m.

The final moisture content of the compressed castor seed, which corresponds to the technological regulation, is reached after 90 min, and the duration of compressed seed processing in each vat is increased by 13 min.

It is known that the main parameter that allows the intensification of the process of moist porous systems' dehydration is the temperature [5] of the heat carrier or that of the heat exchange surface. However, the use of this measure when modifying the process of frying oil-containing raw materials is not advisable since the temperature of compressed castor seed particles in contact with the hot side surface of vats can significantly exceed the maximum permissible temperature of 115 °C.

4. Discussion

The development of modes of moisture–thermal treatment of crushed oilseeds involves a detailed study of the physical processes occurring in the material. This is possible by using mathematical modeling. It should be noted that there is no unified phenomenological

approach to the mathematical modeling of drying, adsorption, and two-phase filtration processes in porous systems so far. The models differ in the number of equations simulating the temperature state of the material and moisture transfer, as well as in the method of determination of the intensity function of phase transformations of liquid and vapor at the internal points of the porous body. The most common methods use the phase transition coefficient [12–15] or the mass transfer equation of the liquid phase [17–25], which require the moisture content function, the correct determination of which, without knowing the intensity of the phase transition, is somewhat problematic.

The molecular radiation theory of heat and mass transfer [26,27,29] enabled equations to be obtained for the intensity of phase transformations on the external and internal surfaces of a capillary–porous body and for the diffusion coefficient of a liquid, which take into account the activation nature of these processes. The function for the contact surface area of the liquid and vapor phases in pores incompletely filled with liquid allowed the inclusion of the influence of body moisture on the intensity of phase transformations during drying and adsorption. The equation for equilibrium vapor pressure enabled the determination of the dynamics of changes in the relative humidity of vapor in the pores of the body.

The applied numerical method allowed the joint solution of the system of Equations (2)–(5) under boundary conditions (12)–(18), considering the mutual influence of heat and mass transfer processes.

The creation of any industrial technology has an accepted scheme: conducting research accompanying the technology (physical or mathematical modeling); approbation of the technology in industrial conditions; and clarification of constitutive parameters based on which the mathematical model or the results of experimental research obtained in the lab are processed.

5. Conclusions

A general mathematical model and numerical method for the calculation of the dynamics and kinetics of heat and mass transfer, and phase transformations, during the wet–heat treatment of raw oil material in a continuous multi-vat brazier were developed. This allows us to define the temperature range, volume concentrations, and partial pressure of the liquid, vapor, and air phases in the dispersed layer, but also the time of humidification and drying. Verification of the results for the compressed seed of the castor plant confirmed the adequacy of the mathematical model and the effectiveness of the numerical method. This testifies to the possibility of their application in the determination of necessary regime parameters, which allow the temperature and humidity indicators for ground oilseeds required by the wet–heat treatment regulations to be reached while taking into account the design characteristics of the brazier.

Author Contributions: Conceptualization, V.D.; methodology, N.S.; software, N.S.; validation, N.S. and V.D.; formal analysis, M.V.; investigation, N.S., V.D. and M.V.; resources, V.D. and M.V.; data curation, V.D.; writing—original draft preparation, N.S.; writing—review and editing, V.D. and M.V.; visualization, M.V.; supervision, N.S.; project administration, V.D. and M.V.; funding acquisition, V.D. and M.V. All authors have read and agreed to the published version of the manuscript.

Funding: This research received no external funding.

Institutional Review Board Statement: Not applicable.

Informed Consent Statement: Not applicable.

Data Availability Statement: Data are contained within the article.

Conflicts of Interest: The authors declare no conflict of interest.

References

1. Kabutey, A.; Herak, D.; Ambarita, H.; Sigalingging, R. Modeling of Linear and Non-linear Compression Processes of Sunflower Bulk Oilseeds. *Energies* **2019**, *12*, 2999. [CrossRef]
2. Didur, V.A.; Tkachenko, V.A. Technology of castor-oil plant seeds processing at small-capacity plants. *Bull. Ukr. Branch Int. Acad. Agrar. Educ.* **2014**, *289*, 21–36. Available online: http://www.tsatu.edu.ua/tstt/wp-content/uploads/sites/6/visnyk-uv-mizhnarodnoyi-akademiyi-ahrarnoyi-osvity-vypusk-2-2014-r.pdf (accessed on 2 June 2022). (In Russian).
3. Didur, V.A.; Tkachenko, V.A.; Tkachenko, A.V.; Didur, V.V.; Aseev, A.A. Modeling of hydrodynamic processes in a multi-pot brazier when roasting castor bean mint. *Sci. Bull. NUBIP Ser. Technol. Energy Agric. Ind. APK* **2017**, *262*, 11–26. Available online: http://journals.nubip.edu.ua/index.php/Tekhnica/article/view/9402 (accessed on 2 June 2022). (In Russian).
4. Huzova, I.O.; Atamanyuk, V.M. Mathematical interpretation of dynamics of temperature change during drying of hot monodispersed layer of organic raw materials. *J. Chem. Technol.* **2021**, *28*, 278–288. [CrossRef]
5. Lykov, A.V. *Drying Theory*; Energy: Moscow, Russia, 1968; 472p. Available online: https://www.twirpx.com/file/1241798/ (accessed on 2 June 2022). (In Russian)
6. Shevtsov, A.A.; Drannikov, A.V.; Zvyagintsev, A.M. Mathematical description of the drying process wheat germ in oscillating modes. *News Univ. Food Technol.* **2006**, *5*, 50–52. (In Russian)
7. Frolova, L.N. Development of Scientific and Practical Foundations of Resource-Saving Processes for the Complex Processing of Oilseeds (Theory, Technique and Technology). Ph.D. Thesis, Voronezh State University of Engineering Technologies, Voronezh, Russia, 2016. Available online: https://www.dissercat.com/content/razvitie-nauchno-prakticheskikh-osnov-resursosberegayushchikh-protsessov-kompleksnoi-pererab (accessed on 1 August 2022). (In Russian).
8. Ginzburg, A.S.; Rezchikov, V.A. *Drying of Foodstuffs in a Fluidized Bed*; Food Industry: Moscow, Russia, 1966; 196p. Available online: http://195.20.96.242:5028/khportal/DocDescription?docid=KhHDUHT.BibRecord.8145 (accessed on 17 June 2022). (In Russian)
9. Cardador-Martínez, A.; Pech-Almeida, J.L.; Allaf, K.; Palacios-Rojas, N.; Alonzo-Macías, M.; Téllez-Pérez, C. A Preliminary Study on the Effect of the Instant Controlled Pressure Drop Technology (DIC) on Drying and Rehydration Kinetics of Maize Kernels (*Zea mays* L.). *Foods* **2022**, *11*, 2151. [CrossRef]
10. Berka-Zougali, B.; Ferhat, M.-A.; Hassani, A.; Chemat, F.; Allaf, K.S. Comparative Study of Essential Oils Extracted from Algerian *Myrtus communis* L. Leaves Using Microwaves and Hydrodistillation. *Int. J. Mol. Sci.* **2012**, *13*, 4673. [CrossRef]
11. Aleksanyan, I.Y.; Titova, L.M.; Nugmanov, A.K. Simulation of the process of drying a dispersed material in a fluidized bed. *Tech. Technol. Food Prod.* **2014**, *3*, 96–102. Available online: https://cyberleninka.ru/article/n/modelirovanie-protsessa-sushki-dispersnogo-materiala-v-kipyaschem-sloe/viewer (accessed on 25 July 2022). (In Russian).
12. Didur, V.V.; Tkachenko, A.V.; Tkachenko, V.A.; Didur, V.A. Mathematical model of the process of preparation of oil raw materials in a multiple brutter. *Comm. Mot. Energetics Agric.* **2016**, *18*, 29–35. Available online: https://agro.icm.edu.pl\T1\guilsinglrightagro\T1\guilsinglrightelement\T1\guilsinglright29-35 (accessed on 25 July 2022). (In Russian).
13. Akulich, P.V. *Thermohydrodynamic Processes in Drying Technique*; ITMO im. Lykova: Minsk, Belarus, 2002; 268p.
14. Kotov, B.I.; Bandura, V.N.; Kalinichenko, R.A. Mathematical modeling and identification of heat and mass transfer in plant dispersed material during drying and heating by an ultra-high frequency electromagnetic field. *Energy Autom.* **2018**, *6*, 35–50. Available online: http://nbuv.gov.ua/UJRN/eia_2018_6_6 (accessed on 1 June 2022).
15. Bandura, V.; Kotov, B.; Gyrych, S.; Gricshenko, V.; Kalinichenko, R.; Lysenko, O. Identification of mathematical description of the dynamics of extraction of oil materials in the electric field of high frequency. *Agraarteadus* **2021**, *32*, 8–16. Available online: https://agrt.emu.ee/pdf/2021_1_bandura.pdf (accessed on 3 August 2022).
16. Sokolovskyy, Y.I.; Boretska, I.B.; Gayvas, B.I.; Kroshnyy, I.M.; Nechepurenko, A.V. Mathematical modeling of convection drying process of wood taking into account the boundary of phase transitions. *Math. Modeling Comput.* **2021**, *8*, 830–841. [CrossRef]
17. Akulich, P.V.; Slizhuk, D.S. Heat and Mass Transfer in a Dense Layer during Dehydration of Colloidal and Sorption Capillary-Porous Materials under Conditions of Unsteady Radiation-Convective Energy Supply. *Theor. Found Chem. Eng.* **2022**, *56*, 152–161. [CrossRef]
18. Rudobashta, S.P.; Kartashov, E.M.; Zueva, G.A. Mathematical modeling of convective drying of materials with taking into account their shrinking. *J. Eng. Phys. Thermophys.* **2020**, *93*, 1394–1401. [CrossRef]
19. Xu, Z.; Leong, S.Y.; Farid, M.; Silcock, P.; Bremer, P.; Indrawati Oey, I. Understanding the Frying Process of Plant-Based Foods Pretreated with Pulsed Electric Fields Using Frying Models. *Foods* **2020**, *9*, 949. [CrossRef]
20. Bansal, H.S.; Takhar, P.S.; Maneerote, J. Modeling multiscale transport mechanisms, phase changes and thermomechanics during frying. *Food Res. Int.* **2014**, *62*, 709–717. [CrossRef]
21. Zhang, L.Z. A three- dimensional non-equlibrium model for an intermittent adsorption cooling system. *Sol. Energy* **2000**, *69*, 27–35. [CrossRef]
22. Leong, K.C.; Liu, Y. Numerical study of a combined heat and mass recovery adsorption cooling cycle. *Intern. J. Heat Mass Transf.* **2004**, *47*, 4761–4770. [CrossRef]
23. Keltsev, N.V. *Fundamentals of Sorption Technology*, 2nd ed.; Chemistry: Moscow, Russia, 1984; 590p. (In Russian)
24. Marlinda; Uyun, A.S.; Miyazaki, T.; Ueda, Y.; Akisawa, A. Performance Analysis of a Double-effect Adsorption Refrigeration Cycle with a Silica Gel/Water Working Pair. *Energies* **2010**, *3*, 1704–1720. [CrossRef]
25. Lattieff, F.A.; Atiya, M.A.; Mahdi, J.M.; Majdi, H.S.; Talebizadehsardari, P.; Yaïci, W. Performance Analysis of a Solar Cooling System with Equal and Unequal Adsorption/Desorption Operating Time. *Energies* **2021**, *14*, 6749. [CrossRef]

26. Nikitenko, N.I.; Snezhkin, Y.F.; Sorokovaya, N.N.; Kolchik, Y.N. *Molecular Radiation Theory and Methods for Calculating Heat and Mass Transfer*; Naukova Dumka: Kyiv, Ukraine, 2014; 744p. Available online: http://ittf.kiev.ua/wp-content/uploads/2016/12/nikitenko.pdf (accessed on 12 June 2022). (In Russian)
27. Nikitenko, N.I. Problems of the radiation theory of heat and mass transfer in solid and liquid media. *J. Eng. Phys. Thermophys.* **2000**, *73*, 840–848. [CrossRef]
28. Rudobashta, S.P. *Mass Transfer in Systems with a Solid Phase*; Chemistry: Moscow, Russia, 1980; 248p. Available online: https://www.libex.ru/detail/book796756.html (accessed on 6 July 2022). (In Russian)
29. Nikitenko, N.I.; Snezhkin, Y.F.; Sorokovaya, N.N. Mathematical simulation of heat and mass transfer, phase conversions, and shrinkage for optimization of process of thermolabile materials. *J. Eng. Phys. Thermophys.* **2005**, *78*, 75–89. [CrossRef]
30. Nikitenko, N.I. Investigation of dynamics of evaporation of condensed bodies on the basis of the law of spectral-radiation intensity of particles. *J. Eng. Phys. Thermophys.* **2002**, *75*, 684–692. [CrossRef]
31. Ginzburg, A.S. *Food Drying Technology*; Food Industry: Moscow, Russia, 1976; 248p. (In Russian)
32. Didur, V.V. Mechanical and technological foundations of deep processing of castor seeds in the conditions of a small-tonnage enterprise. Ph.D. Thesis, Dmytro Motornyi Tavri State Agro-Technological University, Melitopol, Ukraine, 6 May 2021. Available online: http://www.tsatu.edu.ua/nauka/n/specializovani-vcheni-radu/specializovana-vchena-rada-d-18-819-01/ (accessed on 7 June 2022). (In Ukrainian).